

Quantum Holography in a Graphene Flake with an Irregular Boundary

Anffany Chen,^{1,2} R. Ilan,³ F. de Juan,⁴ D. I. Pikulin,⁵ and M. Franz^{1,2}

¹*Department of Physics and Astronomy, University of British Columbia, Vancouver, British Columbia V6T 1Z1, Canada*

²*Quantum Matter Institute, University of British Columbia, Vancouver British Columbia V6T 1Z4, Canada*

³*Raymond and Beverly Sackler School of Physics and Astronomy, Tel-Aviv University, Tel-Aviv 69978, Israel*

⁴*Rudolf Peierls Centre for Theoretical Physics, Oxford, 1 Keble Road, OX1 3NP, United Kingdom*

⁵*Station Q, Microsoft Research, Santa Barbara, California 93106-6105, USA*

 (Received 12 February 2018; revised manuscript received 5 May 2018; published 18 July 2018)

Electrons in clean macroscopic samples of graphene exhibit an astonishing variety of quantum phases when strong perpendicular magnetic field is applied. These include integer and fractional quantum Hall states as well as symmetry broken phases and quantum Hall ferromagnetism. Here we show that mesoscopic graphene flakes in the regime of strong disorder and magnetic field can exhibit another remarkable quantum phase described by holographic duality to an extremal black hole in two-dimensional anti-de Sitter space. This phase of matter can be characterized as a maximally chaotic non-Fermi liquid since it is described by a complex fermion version of the Sachdev-Ye-Kitaev model known to possess these remarkable properties.

DOI: [10.1103/PhysRevLett.121.036403](https://doi.org/10.1103/PhysRevLett.121.036403)

Tensions between the laws of quantum mechanics and classical gravity that are emblematic of the extreme environments occurring in the early Universe and near horizons of black holes constitute the most enigmatic mysteries in modern physics. A promising avenue to resolve some of the paradoxes encountered in these studies, such as the black hole information paradox, is the holographic principle [1]. In holographic duality, quantum gravity degrees of freedom in a $(d + 1)$ -dimensional spacetime “bulk” are represented by a many-body system defined on its d -dimensional boundary.

Important new insights into these fundamental questions have been gained recently through the study of the Sachdev-Ye-Kitaev (SYK) model [2,3], which describes a system of N fermions in $(0 + 1)$ dimensions subject to random all-to-all four-fermion interactions and is dual to dilaton gravity in $(1 + 1)$ -dimensional anti-de Sitter (AdS_2) space [4,5]. Despite being maximally strongly interacting, this model is, remarkably, exactly solvable in the limit of large N . It has been shown to exhibit physical properties characteristic of the black hole, including the extensive ground state entropy $S_0 \sim N$, emergent conformal symmetry at low energy, and fast scrambling of quantum information that saturates the fundamental bound on the relevant Lyapunov chaos exponent λ_T . Extensions of this model also show interesting behaviors, including unusual spectral properties [6–8], supersymmetry [9], quantum phase transitions of an unusual type [10–12], quantum chaos propagation [13–15], patterns of entanglement [16,17], and strange metal behavior [18].

In this Letter we propose a simple experimental realization of the SYK model with complex fermions in a

mesoscopic graphene flake with an irregular boundary and subject to a strong applied magnetic field. Unlike the earlier proposals in solid state systems [19,20], which targeted the Majorana fermion version of the model, our proposed device does not require superconductivity or advanced fabrication techniques and should therefore be relatively straightforward to assemble using only the existing technologies. The proposed design is illustrated in Fig. 1. Magnetic field B applied to graphene is known to produce a variety of interesting quantum phases [21–30]. At the noninteracting level the field simply reorganizes the single-particle electron states into Dirac Landau levels with energies [31] $E_n \simeq \pm \hbar v \sqrt{2n(eB/\hbar c)}$ and $n = 0, 1, \dots$. We argue that when the graphene flake is sufficiently small and irregular the electrons in the $n = 0$ Landau level (LL_0) are generically described by the SYK model. This remarkable property is rooted in the celebrated Aharonov-Casher

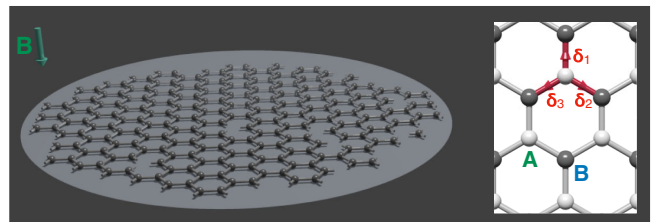


FIG. 1. Schematic depiction of the proposed device. Irregular shaped graphene flake in applied magnetic field B forms the $(0 + 1)$ -dimensional many-body system equivalent to a black hole in $(1 + 1)$ anti-de Sitter space. Inset: lattice structure of graphene with A and B sublattices marked and nearest neighbor vectors denoted by δ_j .

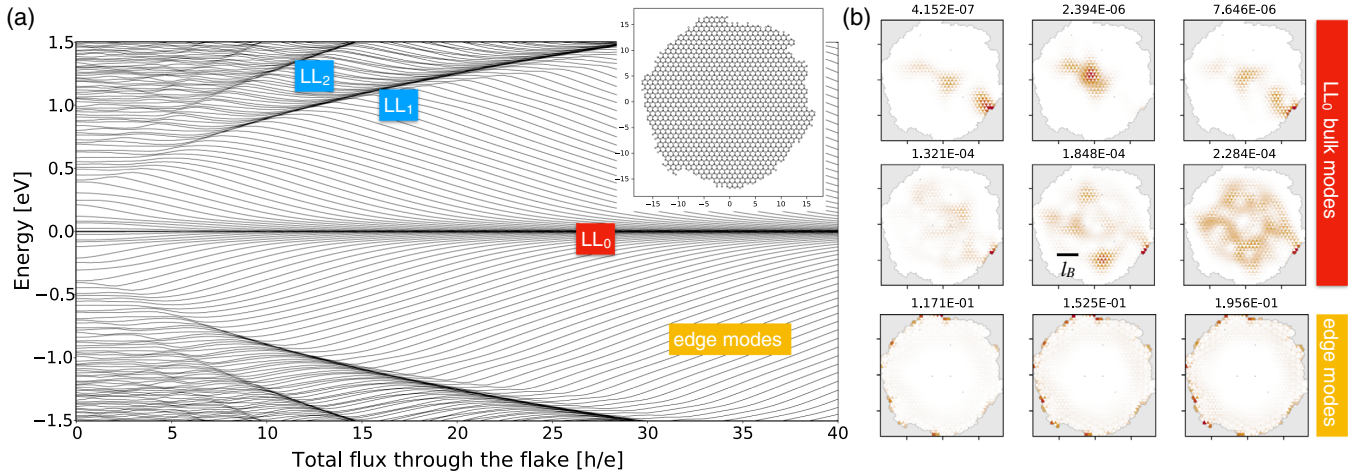


FIG. 2. Electronic properties of an irregular graphene flake in the absence of interactions. (a) Single-particle energy levels ϵ_j of the Hamiltonian H_0 as a function of the magnetic flux $\Phi = SB$ through the flake. The flake used for this calculation, depicted in the inset, consists of 1952 carbon atoms with equal number of A and B sites. The energy spectrum, calculated here in the Landau gauge $\mathbf{A} = Bx\hat{y}$ and with open boundary conditions, shows the same generic features irrespective of the detailed flake geometry. (b) Typical wave function amplitudes of the eigenstates $\Phi_j(\mathbf{r})$ belonging to LL_0 at $\Phi = 40\Phi_0$ and the edge modes. The numerals above each panel denote the energy ϵ_j of the state in eV, scale bar shows the magnetic length $l_B = \sqrt{\hbar c/eB}$.

construction [32] which implies that, in the absence of interactions, LL_0 remains perfectly sharp even in the presence of strong disorder that respects the chiral symmetry of graphene. As we shall see, a flake with a highly irregular boundary, illustrated in Fig. 1, is chirally symmetric. Electrons in LL_0 , therefore, remain nearly perfectly degenerate, despite the fact that their wave functions acquire random spatial structure. When Coulomb repulsion is projected onto these highly disordered states, random all-to-all interactions between the zero modes are generated, exactly as required to define the SYK model.

The complex fermion SYK model, also known as the Sachdev-Ye (SY) model [2,33–35], is defined by the second-quantized Hamiltonian

$$\mathcal{H}_{\text{SY}} = \sum_{ij:kl} J_{ij:kl} c_i^\dagger c_j^\dagger c_k c_l - \mu \sum_j c_j^\dagger c_j, \quad (1)$$

where c_j^\dagger creates a spinless fermion, $J_{ij:kl}$ are zero-mean complex random variables satisfying $J_{ij:kl} = J_{kl:ij}^*$ and $J_{ij:kl} = -J_{ji:kl} = -J_{ij:lk}$ and μ denotes the chemical potential. In what follows we derive the effective low-energy Hamiltonian for electrons in LL_0 of a graphene flake with an irregular boundary and show that, under a broad range of conditions, it is given by Eq. (1). The system, therefore, realizes the SY model.

At the noninteracting level a flake of graphene is described by a simple tight-binding Hamiltonian [31]

$$H_0 = -t \sum_{\mathbf{r}, \delta} (a_{\mathbf{r}}^\dagger b_{\mathbf{r}+\delta} + \text{H.c.}), \quad (2)$$

where $a_{\mathbf{r}}^\dagger (b_{\mathbf{r}+\delta}^\dagger)$ denotes the creation operator of the electron on the sublattice A (B) of the honeycomb lattice.

These satisfy the canonical anticommutation relations $\{a_{\mathbf{r}}^\dagger, a_{\mathbf{r}'}\} = \{b_{\mathbf{r}}^\dagger, b_{\mathbf{r}'}\} = \delta_{\mathbf{r}\mathbf{r}'}$ appropriate for fermion operators. \mathbf{r} extends over the sites in sublattice A , while δ denotes the 3 nearest neighbor vectors (inset Fig. 1). $t = 2.7$ eV is the tunneling amplitude [36]. For simplicity, we first ignore electron spin but reintroduce it later. The chiral symmetry χ is generated by setting $(a_{\mathbf{r}}, b_{\mathbf{r}}) \rightarrow (-a_{\mathbf{r}}, b_{\mathbf{r}})$ for all \mathbf{r} , which has the effect of flipping the sign of the Hamiltonian $H_0 \rightarrow -H_0$.

Magnetic field B is incorporated in the Hamiltonian (2) by means of the standard Peierls substitution, which replaces $t \rightarrow t_{\mathbf{r}, \mathbf{r}+\delta} = t \exp[-i(e/\hbar c) \int_{\mathbf{r}}^{\mathbf{r}+\delta} \mathbf{A} \cdot d\mathbf{l}]$, where \mathbf{A} is the vector potential $\mathbf{B} = \nabla \times \mathbf{A}$. In the presence of χ the Aharonov-Casher construction [32] implies $N = N_\Phi$ exact zero modes in the spectrum of H_0 , where $N_\Phi = SB/\Phi_0$ denotes the number of magnetic flux quanta $\Phi_0 = hc/e$ piercing the area S of the flake. It is clear that a flake with an arbitrary shape described by H_0 respects χ , which underlies the robustness of LL_0 invoked above.

Hopping t' between second neighbor sites and random on-site potential are examples of perturbations that break χ and are therefore expected to broaden LL_0 . These effects can be modeled by adding to \mathcal{H}_{SY} defined in Eq. (1) a term

$$\mathcal{H}_2 = \sum_{ij} K_{ij} c_i^\dagger c_j, \quad (3)$$

which describes a small (undesirable) hybridization between the states in LL_0 that will generically be present in any realistic experimental realization. We discuss the effect of these terms below.

In Fig. 2(a) we show the single-particle energy spectrum of H_0 for a graphene flake with a shape depicted in the

inset. As a function of increasing magnetic field B we observe new levels joining the zero-energy manifold LL_0 such that the number of zero modes follows $N \simeq N_\Phi$ in accordance with the Aharonov-Casher argument. Higher Landau levels and topologically protected edge modes are also visible. Despite the randomness introduced by the irregular boundary LL_0 remains sharp as expected on the basis of the arguments presented above. This is the key feature in our construction of the SY Hamiltonian which guarantees that the \mathcal{H}_2 term defined above vanishes as long as the chiral symmetry is respected. In the presence of e-e repulsion the leading term in the effective description of LL_0 will therefore be a four-fermion interaction which we discuss next.

Electron wave functions $\Phi_j(\mathbf{r})$ belonging to LL_0 exhibit random spatial structure [Fig. 2(b)] owing to the irregular confining geometry imposed by the shape of the flake. From the knowledge of the wave functions it is straightforward to evaluate the corresponding interaction matrix elements (Supplemental Material, Sec. A [37]) between the zero modes. The leading many-body Hamiltonian for electrons in LL_0 will thus have the form of Eq. (1) with

$$J_{ij;kl} = \frac{1}{2} \sum_{\mathbf{r}_1, \mathbf{r}_2} [\Phi_i(\mathbf{r}_1) \Phi_j(\mathbf{r}_2)]^* V(\mathbf{r}_1 - \mathbf{r}_2) [\Phi_k(\mathbf{r}_1) \Phi_l(\mathbf{r}_2)], \quad (4)$$

where $V(\mathbf{r}) = (e^2/\epsilon r) e^{-r/\lambda_{TF}}$ is the screened Coulomb potential with Thomas-Fermi length λ_{TF} and dielectric constant ϵ . The summation extends over all sites of the honeycomb lattice. It is to be noted that only the part of $J_{ij;kl}$ antisymmetric in (i, j) and (k, l) contributes to the many-body Hamiltonian (1) so in the following we assume that $J_{ij;kl}$ has been properly antisymmetrized.

We numerically evaluated $J_{ij;kl}$ for various values of λ_{TF} . The resulting J s are complex valued random variables satisfying

$$\overline{J_{ij;kl}} = 0, \quad \overline{|J_{ij;kl}|^2} = \frac{1}{2N^3} J^2, \quad (5)$$

where J measures the interaction strength and the bar denotes averaging over randomness introduced by the irregular confining geometry. Figure 3(a) shows the statistical distribution of $J_{ij;kl}$ calculated for the nearest-neighbor interactions $V(\mathbf{r}) = V_1 \sum_{\delta} \delta_{\mathbf{r}, \delta}$ and the single-particle wave functions $\Phi_j(\mathbf{r})$ depicted in Fig. 2(b). The distribution of $J_{ij;kl}$ shows the expected randomness with some deviations from the ideal Gaussian.

To ascertain the effect of these deviations and to prove that the low-energy fermions in the graphene flake are described by the SY model we next perform numerical diagonalization of the many-body Hamiltonian (1) with coupling constants $J_{ij;kl}$ obtained as described above. We then calculate various physical observables and compare them to the results obtained with random independent $J_{ij;kl}$.

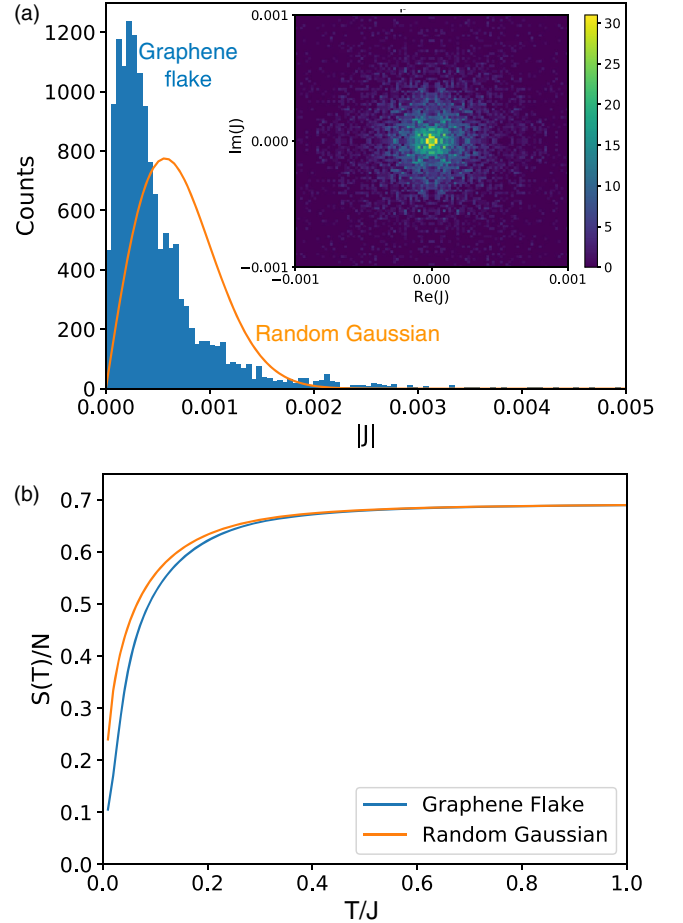


FIG. 3. Statistical properties of the coupling constants and the thermal entropy. (a) Histogram of $|J_{ij;kl}|$ as calculated from Eq. (4) with $V_1 = 1$ for the graphene flake depicted in Fig. 2 and $N = 16$, compared to the Gaussian distribution (orange line) with the same variance $0.000805V_1$. Inset shows the histogram of real and imaginary components of $J_{ij;kl}$. The mirror symmetry about the horizontal follows from the Hermiticity property $J_{ij;kl} = J_{kl;ij}^*$. (b) Entropy $S(T)$ of the SY Hamiltonian (1) calculated with J s shown in panel (a).

Figure 3(b) shows the thermal entropy $S(T)$ of the flake. Comparison to the entropy calculated with random Gaussian $J_{ij;kl}$ indicates no significant difference. It is to be noted that while the SY model is known to exhibit nonzero ground state entropy per particle in the thermodynamic limit, $S(T)$ still vanishes as $T \rightarrow 0$ for any finite N [38].

Many-body energy level statistics provide another useful tool to validate our hypothesis that LL_0 electrons in the graphene flake behave according to the SY model. We thus arrange the energy eigenvalues E_n of the many-body Hamiltonian (1) in increasing order and form ratios of the subsequent levels $r_n = (E_{n+1} - E_n)/(E_n - E_{n-1})$. According to the random matrix theory applied to the SY model [6] probability distributions $P(\{r_n\})$ are given by different Gaussian ensembles, depending on $N \pmod{4}$

TABLE I. Gaussian ensembles for the SY model. The relevant probability distributions are given by Eq. (6) with $Z = (8/27), (4\pi/81\sqrt{3}), (4\pi/729\sqrt{3})$ and $\beta = 1, 2, 4$ for GOE, GUE, and GSE, respectively.

$N(\bmod 4)$	0	1	2	3
$q = 0$	GOE		GSE	
$q \neq 0$	GUE	GUE	GUE	GUE

and the eigenvalue q of the total charge operator $Q = \sum_j (c_j^\dagger c_j - 1/2)$ as summarized in Table I. Here GOE, GUE, and GSE stand for Gaussian orthogonal, unitary, and symplectic ensembles, respectively, and

$$P(r) = \frac{1}{Z} \frac{(r + r^2)^\beta}{(1 + r + r^2)^{1+3\beta/2}}, \quad (6)$$

with constants Z and β listed in Table I. Since \mathcal{H}_{SY} commutes with Q it can be block diagonalized in sectors with definite charge eigenvalue q . As emphasized in Ref. [6] the level statistics analysis must be performed separately for each q sector. Note that q has integer (half-integer) values for N even (odd) and this is why the neutrality condition $q = 0$ can be met only for even values of N . Also note that $q = 0$ corresponds to $N/2$ particles.

Figure 4 shows our results for the level statistics performed for a graphene flake with $N = 14$ through 18 and various values of q . The obtained level spacing distributions are seen to unambiguously follow the prediction of the random matrix theory for the SY model summarized in Table I. We are thus led to conclude that interacting electrons in LL_0 of a graphene flake with an irregular boundary indeed exhibit spectral properties characteristic of the SY model.

In the rest of this Letter we discuss various aspects of the problem relevant to the laboratory realization. Electrons in graphene possess spin which we so far ignored. Given the weak spin-orbit coupling in graphene we may model the noninteracting system by two copies of the Hamiltonian Eq. (2) plus the Zeeman term, $H = H_0 + g^* \mu_B \mathbf{B} \cdot \mathbf{S}_{\text{tot}}$, where \mathbf{S}_{tot} is the total spin operator and $\mu_B = 5.78 \times 10^{-5}$ eV/T is the Bohr magneton. For graphene on the SiO_2 or hBN substrate we may take $g^* \simeq 2$ which gives the bare Zeeman splitting $\Delta E_S(B) \simeq 0.12$ meV/T, or about 2.4 meV at $B = 20$ T. We expect this relatively small spin splitting to be significantly enhanced by the exchange effect of the Coulomb repulsion. The strength of the exchange splitting $\Delta E_C \simeq 8.8$ meV/T is estimated in the Supplemental Material, Sec. A [37]. For such a large spin splitting one may focus on a partially filled LL_0 for a single spin projection and disregard the other. The spinless model considered so far should therefore serve as an excellent approximation of the physical system in the strong field.

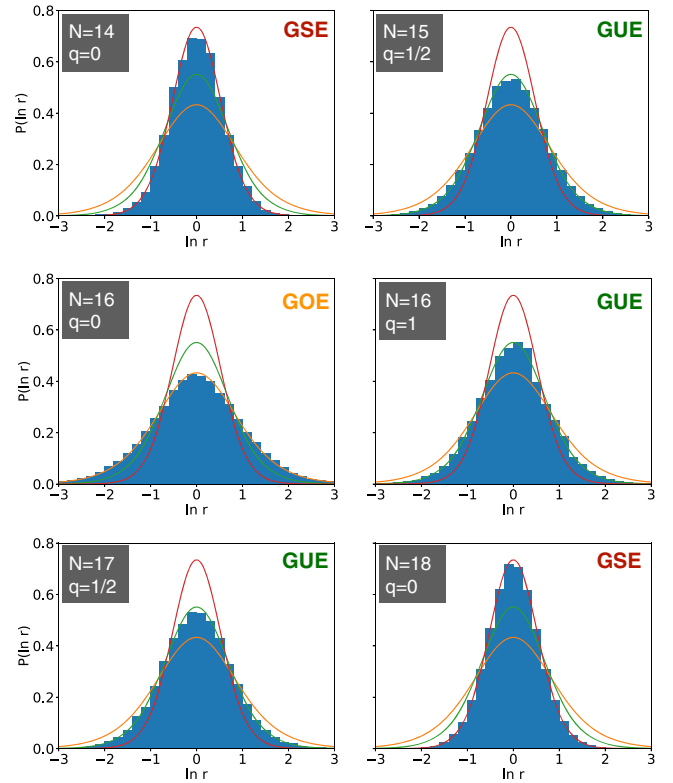


FIG. 4. Many-body level statistics for the interacting electrons in LL_0 of the graphene flake. Blue bars show the calculated distributions for the graphene flake. Orange, green and red curves indicate the expected distributions given by Eq. (6) for GOE, GUE, and GSE, respectively. To obtain smooth distributions, results for $N = 14, 15, 16$ have been averaged over 8 (4) distinct flake geometry realizations while $N = 17, 18$ reflect a single realization.

Disorder that breaks chiral symmetry will inevitably be present in real graphene samples. Such disorder tends to broaden LL_0 and compete with the interaction effects that underlie the SY physics. It is known that bilinear terms \mathcal{H}_2 that arise from such disorder constitute a relevant perturbation to \mathcal{H}_{SY} and drive the system towards a disordered Fermi liquid (dFL) ground state. In the Supplemental Material, Sec. B [37] we analyze the symmetry-breaking effects and estimate their strength in realistic situations. We conclude that in carefully prepared samples a significant window should remain open at nonzero temperatures and frequencies in which the system exhibits behavior characteristic of the SY model.

An ideal sample to observe the SY physics is a graphene flake with a highly irregular boundary and clean interior. These conditions promote random spatial structure of the electron wave functions and preserve degeneracy of LL_0 . Disordered wave functions give rise to random interaction matrix elements $J_{ij;kl}$ while near degeneracy of states in LL_0 guarantees that the two-fermion term \mathcal{H}_2 remains small. To observe signatures of the emergent black hole the

LL_0 degeneracy $N = SB/\Phi_0$ must be reasonably large—numerical simulations indicate that $N \gtrsim 10$ is required for the system to start showing the characteristic spectral features. Aiming at $N \simeq 100$, which is well beyond what one can conceivably simulate on a computer, implies the characteristic sample size $L \simeq \sqrt{S} = \sqrt{N\Phi_0/B} \simeq 150$ nm at $B = 20$ T. Signatures of the SY physics can be observed spectroscopically, e.g., by the differential tunneling conductance $g(V) = dI/dV$ which is predicted [19] to exhibit a characteristic square-root divergence $g(V) \sim |V|^{-1/2}$ in the SY regime at large N , easily distinguishable from the dFL behavior $g(V) \sim \text{const}$ at small V . We predict that a tunneling experiment will observe the SY behavior when the chemical potential of the flake is tuned to lie in LL_0 and dFL behavior for all LL_n with $n \neq 0$. We also expect the two-terminal conductance across the flake to show interesting behavior in the SY regime but we defer a detailed discussion of this to future work.

In the limit of a large flake the irregular boundary will eventually become unimportant for the electrons in the bulk interior and the system should undergo a crossover to a more conventional “clean” phenomenology characteristic of graphene in applied magnetic field. The exact nature of this crossover poses an interesting theoretical as well as experimental problem which we also leave to future study.

The authors are indebted to Ian Affleck, Oguzhan Can, Étienne Lantagne-Hurtubise, and Chengshu Li for stimulating discussions. The work was supported by NSERC, CIFAR (A. C., M. F.) and by the European Union’s Horizon 2020 research and innovation program under the Marie-Sklodowska Curie Grant Agreement No. 705968 (F. J.). Tight-binding simulations were performed using the KWANT code [39] and computational resources provided by WestGrid.

[1] R. Bousso, *Rev. Mod. Phys.* **74**, 825 (2002).
 [2] S. Sachdev and J. Ye, *Phys. Rev. Lett.* **70**, 3339 (1993).
 [3] A. Kitaev, *Proceedings of the KITP Strings Seminar and Entanglement 2015 Program* (Kavli Institute for Theoretical Physics, Santa Barbara, 2015), <http://online.kitp.ucsb.edu/online/entangled15/>.
 [4] S. Sachdev, *Phys. Rev. X* **5**, 041025 (2015).
 [5] J. Maldacena and D. Stanford, *Phys. Rev. D* **94**, 106002 (2016).
 [6] Y.-Z. You, A. W. W. Ludwig, and C. Xu, *Phys. Rev. B* **95**, 115150 (2017).
 [7] J. Polchinski and V. Rosenhaus, *J. High Energy Phys.* **02** (2016) 004.
 [8] A. M. García-García and J. J. M. Verbaarschot, *Phys. Rev. D* **94**, 126010 (2016).
 [9] W. Fu, D. Gaiotto, J. Maldacena, and S. Sachdev, *Phys. Rev. D* **95**, 026009 (2017).
 [10] S. Banerjee and E. Altman, *Phys. Rev. B* **95**, 134302 (2017).

[11] Z. Bi, C.-M. Jian, Y.-Z. You, K. A. Pawlak, and C. Xu, *Phys. Rev. B* **95**, 205105 (2017).
 [12] E. Lantagne-Hurtubise, C. Li, and M. Franz, *Phys. Rev. B* **97**, 235124 (2018).
 [13] Y. Gu, X.-L. Qi, and D. Stanford, *J. High Energy Phys.* **05** (2017) 125.
 [14] M. Berkooz, P. Narayan, M. Rozali, and J. Simón, *J. High Energy Phys.* **01** (2017) 138.
 [15] P. Hosur, X.-L. Qi, D. A. Roberts, and B. Yoshida, *J. High Energy Phys.* **02** (2016) 004.
 [16] C. Liu, X. Chen, and L. Balents, *Phys. Rev. B* **97**, 245126 (2018).
 [17] Y. Huang and Y. Gu, [arXiv:1709.09160](https://arxiv.org/abs/1709.09160).
 [18] X.-Y. Song, C.-M. Jian, and L. Balents, *Phys. Rev. Lett.* **119**, 216601 (2017).
 [19] D. I. Pikulin and M. Franz, *Phys. Rev. X* **7**, 031006 (2017).
 [20] A. Chew, A. Essin, and J. Alicea, *Phys. Rev. B* **96**, 121119 (2017).
 [21] K. S. Novoselov, A. K. Geim, S. V. Morozov, D. Jiang, M. I. Katsnelson, I. V. Grigorieva, S. V. Dubonos, and A. A. Firsov, *Nature (London)* **438**, 197 (2005).
 [22] Y. Zhang, Y.-W. Tan, H. L. Stormer, and P. Kim, *Nature (London)* **438**, 201 EP (2005).
 [23] K. S. Novoselov, Z. Jiang, Y. Zhang, S. V. Morozov, H. L. Stormer, U. Zeitler, J. C. Maan, G. S. Boebinger, P. Kim, and A. K. Geim, *Science* **315**, 1379 (2007).
 [24] K. I. Bolotin, F. Ghahari, M. D. Shulman, H. L. Stormer, and P. Kim, *Nature (London)* **462**, 196 (2009).
 [25] X. Du, I. Skachko, F. Duerr, A. Luican, and E. Y. Andrei, *Nature (London)* **462**, 192 (2009).
 [26] C. R. Dean, A. F. Young, P. Cadden-Zimansky, L. Wang, H. Ren, K. Watanabe, T. Taniguchi, P. Kim, J. Hone, and K. L. Shepard, *Nat. Phys.* **7**, 693 (2011).
 [27] B. E. Feldman, B. Krauss, J. H. Smet, and A. Yacoby, *Science* **337**, 1196 (2012).
 [28] K. Nomura and A. H. MacDonald, *Phys. Rev. Lett.* **96**, 256602 (2006).
 [29] J. Alicea and M. P. A. Fisher, *Phys. Rev. B* **74**, 075422 (2006).
 [30] F. Amet, A. J. Bestwick, J. R. Williams, L. Balicas, K. Watanabe, T. Taniguchi, and D. Goldhaber-Gordon, *Nat. Commun.* **6**, 5838 (2015).
 [31] A. H. Castro Neto, F. Guinea, N. M. R. Peres, K. S. Novoselov, and A. K. Geim, *Rev. Mod. Phys.* **81**, 109 (2009).
 [32] Y. Aharonov and A. Casher, *Phys. Rev. A* **19**, 2461 (1979).
 [33] J. French and S. Wong, *Phys. Lett. B* **33**, 449 (1970).
 [34] O. Bohigas and J. Flores, *Phys. Lett. B* **34**, 261 (1971).
 [35] O. Bohigas and J. Flores, *Phys. Lett. B* **35**, 383 (1971).
 [36] Y. J. Song, A. F. Otte, Y. Kuk, Y. Hu, D. B. Torrance, P. N. First, W. A. de Heer, H. Min, S. Adam, M. D. Stiles *et al.*, *Nature (London)* **467**, 185 (2010).
 [37] See Supplemental Material at <http://link.aps.org/supplemental/10.1103/PhysRevLett.121.036403> for details of our calculations of the interaction matrix elements, the exchange splitting and the chiral symmetry breaking perturbations.
 [38] W. Fu and S. Sachdev, *Phys. Rev. B* **94**, 035135 (2016).
 [39] C. W. Groth, M. Wimmer, A. R. Akhmerov, and X. Waintal, *New J. Phys.* **16**, 063065 (2014).